

Increased levels of RECQ5 shift DNA repair from canonical to alternative pathways

Henry C. Olson^{1,†}, Luther Davis^{2,†}, Kostantin Kiianitsa², Kevin J. Khoo^{1,2}, Yilun Liu³, Theo A. Knijnenburg⁴ and Nancy Maizels^{1,2,*}

¹Department of Biochemistry, University of Washington, 1959 NE Pacific St., Seattle, WA 98195, USA, ²Department of Immunology, University of Washington, 1959 NE Pacific St., Seattle, WA 98195, USA, ³Department of Cancer Genetics and Epigenetics, Beckman Research Institute, City of Hope, 1500 E. Duarte Road, Duarte, CA 91010, USA and ⁴Institute for Systems Biology, 401 Terry Ave. N., Seattle, WA 98109, USA

Received January 02, 2018; Revised July 28, 2018; Editorial Decision July 30, 2018; Accepted August 02, 2018

ABSTRACT

RECQ5 (RECQL5) is one of several human helicases that dissociates RAD51–DNA filaments. The gene that encodes RECQ5 is frequently amplified in human tumors, but it is not known whether amplification correlates with increased gene expression, or how increased RECQ5 levels affect DNA repair at nicks and double-strand breaks. Here, we address these questions. We show that RECQ5 gene amplification correlates with increased gene expression in human tumors, by *in silico* analysis of over 9000 individual tumors representing 32 tumor types in the TCGA dataset. We demonstrate that, at double-strand breaks, increased RECQ5 levels inhibited canonical homology-directed repair (HDR) by double-stranded DNA donors, phenocopying the effect of BRCA deficiency. Conversely, at nicks, increased RECQ5 levels stimulated ‘alternative’ HDR by single-stranded DNA donors, which is normally suppressed by RAD51; this was accompanied by stimulation of mutagenic end-joining. Even modest changes (2-fold) in RECQ5 levels caused significant dysregulation of repair, especially HDR. These results suggest that in some tumors, RECQ5 gene amplification may have profound consequences for genomic instability.

INTRODUCTION

The importance of RECQ5 (RECQL5) helicase in maintaining genomic stability is well established. RECQ5 interacts with MRE11 (1) and is recruited by the MRE11–RAD50–NBS1 complex to double-strand breaks (DSBs). RECQ5 removes RAD51 filaments from stalled replication forks in mitosis to allow cleavage by MUS81 that en-

ables DNA-repair synthesis and corrects chromosome segregation (2). RECQ5 also interacts with RNA Pol II to regulate the rate of transcription elongation genomewide (3). The absence of RECQ5 activity reduces frequencies of canonical homology-directed repair (HDR) at targeted DSBs (4), and depletion of RECQ5 results in transcription-associated genomic instability (5–9). RECQ5 dissociates RAD51 filaments bound to DNA in a reaction dependent upon RECQ5 helicase adenosine triphosphatase (ATPase) activity and interaction with RAD51 *in vitro* (10–13). BLM and FANCD1 helicases can also dissociate RAD51 filaments (4,14,15), but RECQ5 is distinguished by its rapid relocalization in response to exogenous damage that results in either nicks or DSBs (16–18).

Mutation of RECQ5 has not been directly associated with predisposition to cancer or genetic disease, in contrast to two other RECQ family helicases, BLM and WRN (19). However, amplification of the RECQ5 gene occurs frequently (20–24). RECQ5 gene amplification characterizes 20–25% of breast cancers and neuroendocrine prostate cancers, and it is the predominant form of RECQ5 gene alteration in many cancers (Figure 1A and Supplementary Figure S1). The genes encoding FANCD1 and BLM helicases are also frequently amplified in tumors, while the gene encoding WRN is more frequently altered by deletion or mutation (Figure 1A). Gene amplification is predicted to result in increased levels of RECQ5, but neither that prediction nor the consequences of increased RECQ5 levels for DNA repair have been examined systematically.

Some HDR pathways depend upon RAD51–DNA filaments formed at a DNA break to enable invasion of a homologous duplex DNA donor (25–28). These ‘canonical’ HDR pathways contrast with ‘alternative’ HDR pathways, which may be independent of or even suppressed by RAD51 [(11,26,28–38) reviewed by (39)]. An especially clear example of alternative HDR is evident at nicks, where HDR supported by exogenous single-stranded DNA (ss-

*To whom correspondence should be addressed. Tel: +1 206 221 6876; Fax: +1 206 221 6781; Email: maizels@u.washington.edu

†The authors wish it to be known that, in their opinion, the first two authors should be regarded as Joint First Authors.

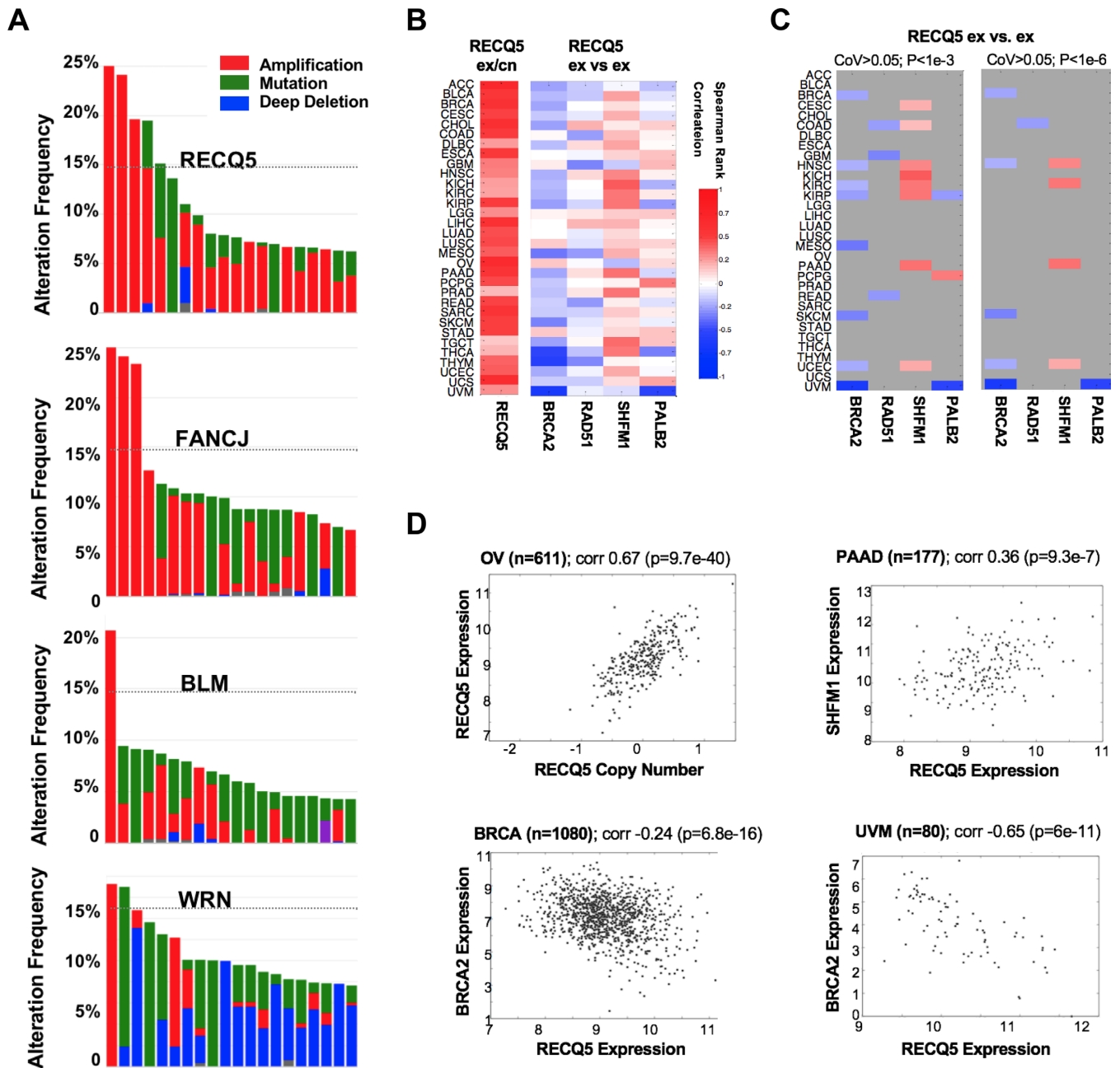


Figure 1. RECQ5 amplification correlates with increased RECQ5 gene expression. (A) Alteration of RECQ5 and other helicases in human cancers. Reduced images of histograms generated at the Memorial Sloan Kettering Cancer Center (MSKCC) cBio Portal (www.cbioportal.org) comparing frequencies of amplification, mutation and deep deletion of four human helicases [RECQ5 (RECQL5), FANCI (BRIP1), BLM and WRN] in the 20 tumors in which alterations in these genes are most frequently found, each represented by a bar. Tumor types are identified and frequencies of amplification in additional tumors shown in the larger images presented in Supplementary Figure S1. Detailed information is available at the MSKCC cBio portal. (B) Heatmap depicting Spearman rank correlation coefficients for the correlation between RECQ5 gene expression (ex) and copy number variation (cn) (left column) and RECQ5 gene expression and the expression of BRCA2, RAD51, SHFM1 (DSS1) and PALB2 (four columns on the right) across 32 different cancer types labeled by their TCGA abbreviations (rows). (C) Two heatmaps depicting Spearman rank correlation coefficients for the correlation between RECQ5 gene expression and the expression of BRCA2, RAD51, SHFM1 (DSS1) and PALB2, as in panel (A). Only statistically significant associations are shown in color—others are gray. The criteria for significance in terms of coefficient of variation (CoV) and *P*-value are shown above the heatmaps, and are $CoV > 0.05$, $P < 1e^{-3}$ and $CoV > 0.05$, $P < 1e^{-6}$ for the left and right heatmaps, respectively. (D) Scatterplots with the Spearman rank correlation and associated *P*-value are printed above the plots. Copy number data are normalized around zero such that two copies corresponds to zero. Plotted are: top left, RECQ5 copy number (*x*-axis) versus RECQ5 gene expression (*y*-axis) for 611 ovarian (OV) tumor samples from TCGA; top right, RECQ5 gene expression (*x*-axis) and expression of SHFM1 (*y*-axis) in 177 pancreatic adenocarcinoma (PAAD) tumor samples; bottom left and right: RECQ5 gene expression (*x*-axis) and expression of BRCA2 (*y*-axis) in 1080 BRCA and 80 UVM tumor samples.

DNA) donors is stimulated dramatically by treatments that limit formation or persistence of RAD51 filaments (40,41). Targeted nicks are useful in genome engineering and gene therapy, as they are repaired with less associated mutagenic end-joining (mutEJ) than targeted DSBs, making it particularly interesting to fully understand pathways of nick repair.

The well-documented ability of RECQ5 to dissociate RAD51 filaments predicts that increased levels of RECQ5 will stimulate alternative HDR at nicks, but diminish canonical HDR at DSBs. Here, we test that prediction. We first show that RECQ5 gene amplification correlates with increased gene expression in human tumors, by *in silico* analysis of 32 tumor types (>9000 individual tumor samples) in the TCGA database. We then ask how changes in RECQ5 protein levels affect frequencies of both HDR and mutEJ at DSBs and nicks targeted by CRISPR/Cas9 and Cas9D10A in human cells. We demonstrate that, as predicted, increased RECQ5 levels inhibit canonical HDR by double-stranded DNA (dsDNA) donors, as also occurs in tumors deficient in the BRCA1 or BRCA2 proteins. Conversely, increased RECQ5 levels stimulate alternative HDR and mutEJ at nicks. The effects of increased RECQ5 levels reflect the ability of RECQ5 to disrupt RAD51 filaments, as they depend upon RECQ5 helicase activity and RAD51 interactions, and are evident only under conditions permissive for RAD51 filament formation. These results show that RECQ5 gene amplification may dysregulate repair by downregulating canonical HDR and stimulating alternative pathways.

MATERIALS AND METHODS

Cell lines, cell culture, gene targeting and HDR donors

Cells were cultured in Dulbecco-modified Eagle's medium (Hyclone) supplemented with 10% fetal bovine serum (Atlanta Biological, Lawrenceville, GA) and 200 units/ml penicillin, 200 µg/ml streptomycin (Hyclone) and 2 mM L-glutamine (Hyclone) at 37°C in 5% CO₂ (40).

The Traffic Light (TL) reporter (42) was stably integrated into the genome of HEK293T cells, an SV40 T antigen-transformed line, which derives from human embryonic kidney; HT1080, a p53+ human fibrosarcoma line, which maintains a predominantly diploid karyotype in culture.

The Cas9 and Cas9^{D10A} expression constructs were previously described (40).

Expression of sgRNAs was from the gRNA cloning vector (<http://www.addgene.org/41824/>) with single guide RNA (sgRNA) sequences cloned as described in (43). Briefly, 60-mer oligos were annealed and extended then cloned using the Gibson Assembly[®] Cloning Kit (NEB). The sgRNAs used to target the TL reporter were (protospacer-associated motifs capitalized):

g1: 5'-gtgtccggcctcgaccgtgAGG

g2: 5'-CCGtgaggaggtttctgtgtaa

g9: 5'-aaagctaagagctcacctaCGG

The dsDNA donor plasmid for correction of the TL reporter, pCVL SFFV d14GFP, was previously described (40). Single-stranded deoxyoligonucleotide (SSO) donors for HDR at the TL reporter were synthetic oligonucleotides

99 nt in length. The two donors for HDR that correct the GFP gene in the TL reporter bear 41-nt regions homologous to the TL reporter flanking a central 17-nt region of heterology that converts the defective GFP reporter to GFP+ upon replacement of the 38-nt sequence insertion in the defective GFP gene target. Their sequences and the sequence of the GFP gene target are shown in Supplementary Figure S2A.

HT1080 cells bearing a disabling mutation in exon 17 of the CD44 gene were constructed to enable assays of HDR at an endogenous gene by flow cytometry. Sequences of the wild-type gene and disabling mutation are shown in Supplementary Figure S2B. CD44 encodes a cell surface glycoprotein that is critical for cell-cell interactions *in vivo* but not for proliferation in culture. The CD44 gene is comprised of 18 exons. Exon 17 encodes the membrane-spanning domain, which must be intact for retention of CD44 on the cell surface. Prior to engineering, the starting population of HT1080 cells (ATCC; Manassas, VA) was confirmed to be diploid by flow cytometry of cells stained with 4',6-Diamidino-2'-phenylindole dihydrochloride (DAPI), and >99% CD44+ as assayed by flow cytometry of cells stained with fluorescein isothiocyanate (FITC)-conjugated anti-CD44 antibody (clone G44-26; BD Bioscience). A disabling mutation was engineered into exon 17 by transfecting cells with CRISPR/Cas9D10A, gRNA-CD44T-17-1 and SSO donor CD44T-17eng1, which replaced 38 bp of exon 17 with the 17-bp sequence shown in lowercase font (see below), thereby converting CD44+ cells to CD44- cells. Four days after transfection, individual CD44- cells were sorted by flow cytometry and cultured in a 96-well plate for 10 days. Clones were then expanded, genomic DNA isolated and the targeted region was polymerase chain reaction-amplified using primers Ex17-F and Ex17-R and sequenced. We then confirmed that the engineered mutation could be corrected by HDR, targeted with gRNA-CD44T-17-2 and supported by donor SSO-CD44T-17-0. Further experiments were carried out with one of the resulting clones, HT1080 K1.

The sgRNAs (protospacer motifs capitalized) used to target the CD44 gene were:

gRNA-CD44T-17-1: 5'-CCAgatgctgatcatcttggc-3'

gRNA-CD44T-17-2: 5'-CCAgagctgaatttagctagc-3'

SSO donors for HDR at the CD44 gene were (homology arms capitalized):or

SSO-CD44T-17-eng1: 5'-CTGAAGCTCACGCATGTC
ATTTAATTTACTCATAACCAGAAgcttgaatttagctagcG
ATTCTTGCAgTTTGCATTGCAGTCAACAGTCG
AAGAAGG-3'

SSO-CD44T-17-0 (matches human CD44 gene, GRCh38 chr 11:35221616-35221733): 5'-CTGAAGCTCACGCAT
GTCATTTAATTTACTCATAACCAGAA
tgctgatcatcttggcatccctcttggccttggcttggattCTTGCAGTTT
GCATTGCAGTCAACAGTCGAAGAAGG-3'

PCR primers were:

Ex17-F: 5'-CTGCCTATTGGCTGGACCTA-3'

Ex17-R: 5'-TGTCTCTAAAAACCGGGGCA-3'

Assays of HDR and mutEJ frequencies

293T TL cells were seeded in 24-well plates at 1×10^5 cells per well in 500 μ l of medium or in 96-well plates at 4×10^3 cells per well in 100 μ l of medium. HT1080 TL and HT1080 K1 cells were seeded in 24-well plates at 5×10^4 cells per well in 500 μ l of medium. At 4 h after seeding, small interfering RNA (siRNA) transfections were carried out with the ThermoFisher RNAiMax kit (final concentration of siRNA 3 nM). At 24 h after seeding, cells were transfected with constructs expressing CRISPR/Cas9, CRISPR/CAS9^{D10A}, RECQ5 expression constructs and dsDNA or SSO donors, as indicated, using the lipofectamine LTX kit (ThermoFisher) as per manufacturer's guidelines. Each 100 μ l of transfection master mix (100 μ l per well in 24-well plates and 20 μ l per well in 96-well plates for all cell lines) contained 150 ng of the Cas9 or Cas9^{D10A} expression construct, 150 ng of donor DNA (SSO or dsDNA), 75 ng of guide RNA expression construct and 50 ng of the construct for expression of RECQ5 or its mutant derivatives, or the corresponding empty vector (E.V.). At 48 h after seeding, cells were expanded from 24-well plates by transfer to 6-well plates in 2.5 ml medium, followed by continued incubation. No transfer was performed for cells initially plated in 96-well plates. Cells were collected at 96 h (293T TL cells) or 120 h (HT1080 cells) after seeding, resuspended in 2% formaldehyde (final concentration 2%), then stored at 4°C in the dark until analysis using an LSR II flow cytometer (Becton Dickinson, Franklin Lakes, NJ).

For flow cytometry, $\sim 10^5$ cells were analyzed for each replicate. Live cells were identified by forward scatter area and linear side scatter area and gated for single cells by subsequent side scatter height by width as discussed in detail elsewhere (44). Data were analyzed using FlowJo software (version 9.6) and replicates then averaged and standard error of the mean calculated using Excel. Significance was determined by a two-tailed *T* test with unequal sample variance. *P* values <0.05 were deemed statistically significant and are indicated in figures. Each experiment was independently performed at least twice on triplicate samples, and results pooled for statistical analysis.

Assays of HDR and mutEJ frequencies at the TL reporter were carried out by flow cytometry analyses of GFP+, mCherry+ and BFP+ cells (488, 561 and 406 nm lasers, respectively) as described (40,41,44). HDR and mutEJ frequencies are reported as a percentage of transfected cells in a population for 293T TL cells and as a percentage of total cells for HT1080 TL. Absence of a donor typically reduced frequencies of GFP+ cells 100-fold or more. Depletion of RAD51 or BRCA2 was monitored by assessing inhibition of canonical HDR at a DSB by a dsDNA donor.

Assays of HDR at exon 17 of the CD44 gene in HT1080 K1 cells were carried out by flow cytometry analyses of formaldehyde-fixed cells. Exon 17 encodes the transmembrane domain of the CD44 cell-surface glycoprotein, and mutation of this domain in HT1080 K1 cells prevents display of the CD44 protein on the cell surface. CD44 was recognized by staining with a FITC-conjugated anti-CD44 monoclonal antibody (clone G44-26; BD Bioscience) that recognizes ectodomain epitope 1, expressed on all isoforms

of CD44. The antibody was diluted 1:300 in phosphate buffered saline (PBS) + 1% fetal bovine serum (FBS) and used to stain cells for 1 h at 4°C. Cells were centrifuged, resuspended in PBS + 1% FBS and immediately analyzed by flow cytometry (FITC, excitation 495 nm; emission 519 nm). HDR frequencies are reported as a percentage of total cells.

Western blots

Cells were seeded in 24-well plates at 1×10^5 cells/well and transfected with RECQ5 variants (six replicates per variant) and a nuclease-dead derivative of Cas9. At 24 h after seeding, cells were transferred to 6-well plates and expanded for 48 h. At 96 h after seeding, two of the six replicates were collected and analyzed via flow cytometry to record transfection efficiency using BFP levels. Populations with <20% transfection efficiency were not analyzed further, nor were experiments in which transfection efficiency deviated by more than 10% between samples. Whole cell extracts were prepared from four replicate wells by extraction with RIPA buffer [20 mM Tris-Cl (pH 7.5), 150 mM NaCl, 1 mM Na₂ ethylenediaminetetraacetic acid (EDTA), 1 mM [ethylene glycol-bis(β-aminoethyl ether)-N,N,N',N'-tetraacetic acid] (EGTA), 1% nonyl phenoxypolyethoxyethanol (NP-40), 1% sodium deoxycholate, 2.5 mM sodium pyrophosphate] supplemented with complete, EDTA-free protease inhibitor cocktail (Roche). Samples were incubated on ice for 10 min, sonicated and centrifuged briefly to remove debris, then 1% of cell lysate supernatant was analyzed on a NuPAGE 4–12% Bis-Tris Gel (Invitrogen). Proteins were transferred to Polyvinylidene fluoride (PVDF) membrane (ThermoFisher), which was washed and then probed with appropriate antibodies as specified by the manufacturer's directions. Primary antibodies used were anti-RECQ5 (8); anti-FLAG (Origene murine monoclonal anti-DDK, clone OTI4C5); anti-α tubulin (rabbit polyclonal, Neomarkers RB-9281-PO) and anti-actin (Santa Cruz goat polyclonal IgG, sc-1616), all at 1:1000 dilution. Secondary detection was carried out using HRP-coupled antibodies: goat anti-rabbit IgG, goat anti-mouse IgG and donkey anti-goat IgG (Santa Cruz, sc-2004, sc-2005 and sc-2020, respectively), all at 1:5000 dilution. Immune complexes were visualized using the ECL system (Pierce).

siRNA depletion

Depletions of RAD51 and BRCA2 were carried out with previously validated siRAD51 (ThermoFisher ID # s11734) and siBRCA2 (ThermoFisher ID # s2085). The non-specific siRNA, siNT2 (ThermoFisher ID #4390847), was used as a control for depletion analyses. Depletion of RAD51 and BRCA2 was confirmed experimentally by a physiological control, establishing that frequencies of canonical HDR diminished in response to depletion (40,41).

Depletion of RECQ5 was tested using three different siRNAs, Ambion Silencer Select s17988, s17989 and s17990 (Thermo-Fisher), which target endogenous RECQ5 exons 2, 3 and 4, respectively. These siRNAs all reduced endogenous RECQ5 levels ~ 3 -fold in 293T TL

cells (Supplementary Figure S3). Treatment with si17988 alone, which is referred to as siRECQ5 herein, was used to deplete endogenous RECQ5 in 293T TL cells not expressing ectopic RECQ5. In 293T TL cells expressing ectopic RECQ5, endogenous RECQ5 was depleted using a custom Stealth siRNA, siRECQ5-St (5'-GCCCAUUGGAAUUAUGCCAAGUCUA), designed to target exon 7 of endogenous RECQ5 but not the FLAG-RECQ5 transcript encoded by the expression vector, which is protected against this siRNA (8). Cells were treated with siRNAs 48 h prior to transfection with the RECQ5 expression construct, collected at 72 h and the RECQ5 signal probed by western blotting. Protection of ectopically expressed FLAG-tagged RECQ5 from siRECQ5-St but not the siRNAs targeting exons 2, 3 or 4 was confirmed by western blotting (Supplementary Figure S3). Effective depletion of ectopically expressed FLAG-tagged RECQ5 by siRECQ5 but not siRECQ5-St was confirmed by Western blots probed with anti-FLAG antibodies (Supplementary Figure S4A).

HT1080 cells were depleted for endogenous RECQ5 by treatment with siRECQ5 for 24 h prior to transfection with nuclease and gRNA expression constructs. In these cells, siRECQ5 treatment reduced endogenous RECQ5 levels 1.9-fold (Supplementary Figure S5). This reduction was sufficient to reduce frequencies of canonical HDR in a physiological assay (Figure 5).

RECQ5 mutants and ectopic protein expression

Clones expressing FLAG-tagged full-length RECQ5 (referred to herein as RECQ5) and the corresponding RECQ5¹⁻⁸⁹⁹ truncation mutant had been modified within exon 7 to confer protection from siRECQ5-St (8). RECQ5 derivatives bearing point mutations were generated starting with the FLAG-tagged parental clone using QuikChange II XL Site-Directed Mutagenesis Kit (Agilent Technologies) as per manufacturer's directions, and amplifying the RECQ5 expression construct with the following primers (single base changes that created the mutations are indicated in lower case and underlined) and their reverse complement:

D157A: 5'-CTTACTTGGTGGTGGcTGAAGCTCAT TGTG;

K598E: 5'-GTGGCCAACCTCTACgAGGCCAGCGT GCTG;

F666A: 5'-CAAAGGCTCCTGCCCGgCCCAGACG GCCAC.

Western blots probed with anti-FLAG antibodies showed that FLAG-RECQ5 and its mutant derivatives were expressed at comparable levels (Supplementary Figure S4B).

Western blots probed with anti-RECQ5 antibodies (8) identified endogenous RECQ5 and FLAG-RECQ5, distinguished by its slightly slower mobility and evident in cells transfected with the FLAG-tagged RECQ5 expression construct but not control transfectants (Supplementary Figures S3 and S5). Based on relative intensities, ectopic expression increased RECQ5 levels 15-fold in 293T TL cells and 1.9-fold in HT1080 TL cells. Transfections with an empty expression vector were carried out as controls for analysis of the effects of ectopic expression of RECQ5.

RESULTS

RECQ5 gene amplification correlates with increased RECQ5 gene expression in human tumors

The RECQ5 gene is frequently amplified in tumors, as are the genes encoding FANCI and BLM helicases, but not the gene encoding WRN helicase [Figure 1A, larger images in Supplementary Figure S1 (21); The Cancer Genome Atlas (TCGA; <http://cancergenome.nih.gov/>)]. It is not known whether RECQ5 amplification correlates with increased RECQ5 gene expression or with dysregulated expression of other genes involved in recombinational repair. To address these questions, we first queried correlations between RECQ5 gene amplification and increased RECQ5 gene expression for 32 cancer types (>9000 individual tumors) obtained from TCGA. TCGA Level 3 data (normalized and gene-level summarized) were downloaded in July 2015 and have not changed since. We found a clear positive correlation in all 32 tumor types queried (Figure 1B). For 22 of these tumor types, the correlation was statistically significant based on the following three criteria: (i) at least 50 samples were available for calculation of the correlation; (ii) the coefficient of variation for both the copy number data and the gene expression data were at least 0.05 and (iii) the uncorrected *P*-value associated with the Spearman rank correlation was below 0.001.

We then asked if increased expression of RECQ5 in individual primary tumors exhibited positive or negative correlation with dysregulated expression of other genes in the RAD51/BRCA2 pathway, including RAD51, BRCA2 and BRCA2-interacting proteins SHFM1(DSS1) and PALB2. Positive correlation was evident only with SHFM1 (DSS1). Applying the same criteria for statistical significance as above, correlation was evident at $P < 1e-3$ and persisted in four tumor types at the relatively stringent criterion of $P < 1e-6$ (Figure 1C). Negative correlations with BRCA2 and PALB2 were evident at $P < 1e-3$ and persisted at the relatively stringent criterion of $P < 1e-6$ in five tumor types (Figure 1C). The negative correlation of RECQ5 with BRCA2 and RAD51 expression suggests that some tumors may adapt to RECQ5 gene amplification by downregulating canonical, RAD51-dependent repair, thereby phenocopying BRCA2 deficiency.

Correlations are plotted for individual examples of tumor types (Figure 1D) to illustrate how RECQ5 gene expression varies with RECQ5 gene copy number in ovarian cancer ($n = 611$), with a Spearman correlation = 0.67 ($P = 9.7e-40$); how RECQ5 gene expression exhibits positive correlation with SHFM1 gene expression in pancreatic adenocarcinoma ($n = 117$; Spearman correlation = 0.36; $P = 9.3e-7$) and to illustrate negative correlations between RECQ5 and BRCA2 expression in breast cancer (BRCA; $n = 1080$; Spearman correlation = -0.24 ; $P = 6.8e-16$) and uveal melanoma (UVM; $n = 80$), where the negative correlation was very highly significant (Spearman correlation = -0.65 ; $P = 6e-11$).

Assays of HDR and mutEJ at targeted nicks and DSBs

Canonical HDR depends on formation of RAD51–DNA filaments to invade duplex DNA donors (Figure 2A, left).

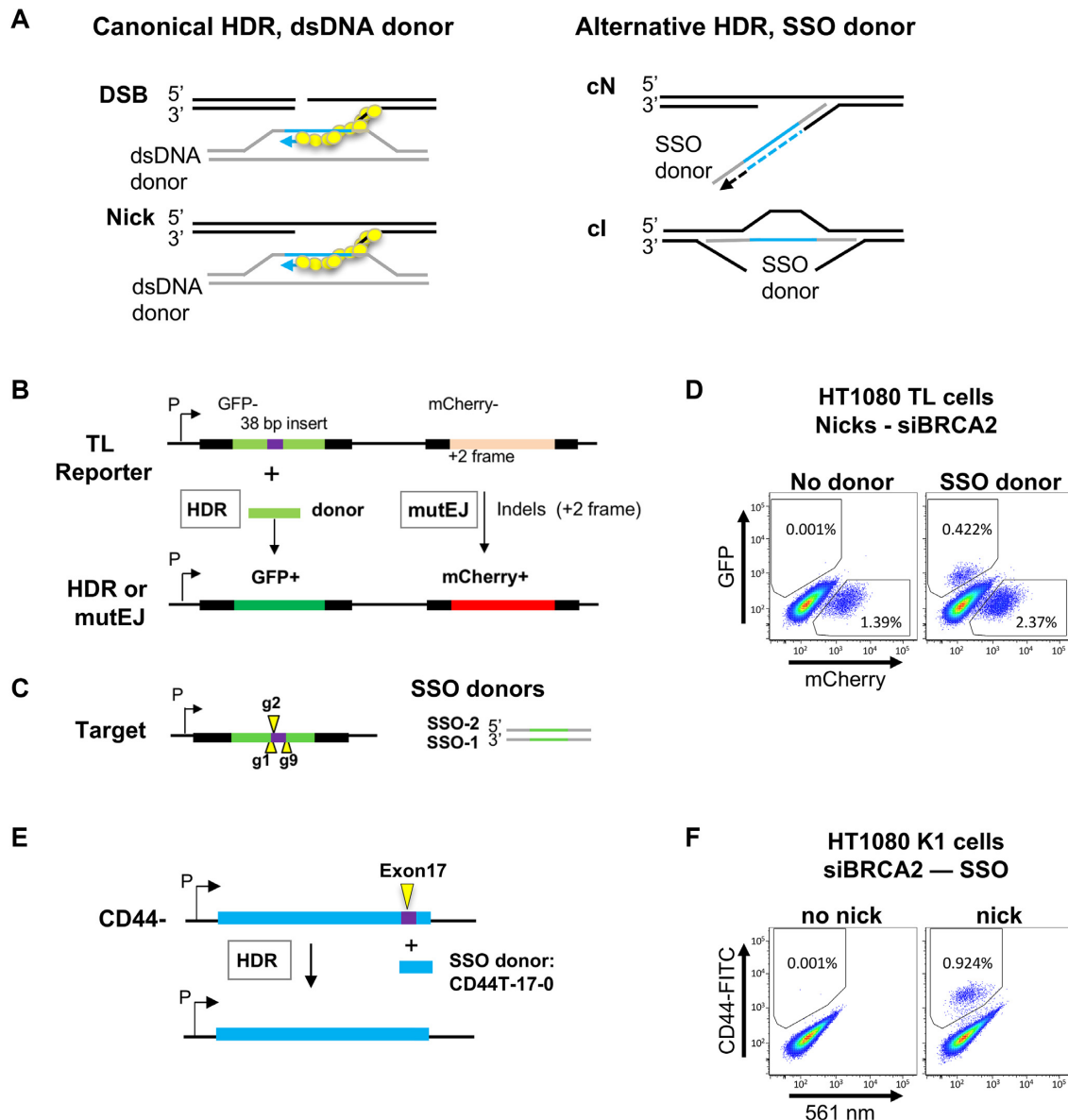


Figure 2. Canonical and alternative HDR pathways, and the TL reporter assay. (A) Diagrams of pathways of canonical and alternative HDR at nicks (top) and DSBs (below) by dsDNA donors (right) or by SSO donors complementary to either the nicked (cN) or intact (cl) strand. (B) The TL reporter assay for HDR and mutEJ (42). In this chromosomal reporter, an SFV promoter (P) drives transcription of a GFP gene (light green) rendered non-functional by insertion of a 38-bp region (purple) containing two premature stop codons, separated by a T2A linker from an mCherry gene (orange) in the +2 reading frame. A targeted nick or DSB (arrowhead) can initiate HDR by a dsDNA or ssDNA donor resulting in GFP+ cells. Alternatively, mutEJ that moves mCherry into the correct reading frame results in mCherry+ cells. For more detailed assay description see (44). (C) Left, the TL target and sites cleaved by gRNAs g1, g2 and g9 that were used to initiate nicks and DSBs in the TL reporter. Right, SSO donors, SSO-1 and SSO-2. (D) Representative quantification of HDR (GFP+) and mutEJ (mCherry+) frequencies in HT1080 TL cells by flow cytometry. Gating and frequency of GFP+ and mCherry+ cells indicated by boxes. (E) Assay of HDR that corrects the disabling mutation in exon 17 of HT1080 TL cells. (F) Representative quantification of HDR frequencies in HT1080 K1 by flow cytometry. A targeted nick initiates HDR by an SSO donor resulting in CD44+ cells, imaged after staining with anti-CD44-FITC antibodies. Gating and frequency of CD44+ (GFP+) cells indicated by boxes.

As RECQ5 disrupts RAD51 filaments, its increased expression is therefore predicted to inhibit canonical HDR by dsDNA donors. In contrast, HDR at nicks by ssDNA donors depends upon alternative pathways in which the target anneals to the donor without strand invasion (Figure 2A, right) and is stimulated by treatments that inhibit formation of RAD51–DNA filaments (40,41). Thus, in-

creased RECQ5 expression is predicted to stimulate alternative HDR by ssDNA donors at nicks.

We tested the effects of RECQ5 overexpression at both the chromosomal TL reporter and an endogenous gene. The TL reporter (42) allows quantification of both HDR and mutEJ resulting from targeted DNA cleavage. It carries a GFP gene disabled by a 38-bp insert (Figure 2B). Nicks or DSBs targeted in or near this insert, at sites recognized by

guide RNAs g1, g2 and g9, can be repaired by HDR using SSOs complementary to the non-transcribed or transcribed strand of the target, respectively [(SSO-1 and SSO-2, respectively, Figure 2B (40,41)]. At nicks targeted by g1 and g9, SSO-1 is complementary to the intact strand and supports HDR by the cI pathway, and SSO-2 is complementary to the nicked strand and supports HDR by the cN pathway, as shown in Figure 2A; conversely, at nicks targeted by g2, SSO-2 supports HDR by the cI pathway and SSO-1 by the cN pathway. HDR using either SSO or duplex DNA donors generates GFP⁺ cells (Figure 2C). The TL reporter also carries an out-of-frame mCherry gene that is shifted into the correct frame by +2 deletions/insertions, generating mCherry⁺ cells (Figure 2C). Thus, frequencies of both HDR and mutEJ can be measured in a single experiment by scoring frequencies of GFP⁺ and mCherry⁺ cells. Figure 2D presents a representative example of assays in HT1080 TL cells that quantify HDR and mutEJ by using flow cytometry to score GFP⁺ and mCherry⁺ cells.

To assay HDR frequencies at an endogenous gene, we engineered a derivative of HT1080 cells carrying a mutation in exon 17 of the CD44 gene. HT1080 is a p53⁺ human fibrosarcoma line that maintains a largely diploid karyotype during proliferation in cell culture, allowing analysis of HDR at an endogenous gene without complications due to polyploidy. The CD44 gene encodes a cell surface glycoprotein that is expressed on most cells and required for development *in vivo* but not for proliferation in cell culture. HT1080 cells stained with anti-CD44 antibodies are CD44⁺ by flow cytometry. HT1080 K1 cells carry a mutation at exon 17 that prevents CD44 expression, which is corrected by HDR at a nick targeted to CD44 exon 17 by gRNA-CD44T-17-2 and supported by the SSO donor CD44T-17-0 (Figure 2E and Supplementary Figure S2B). Gene correction converts cells from CD44⁻ to CD44⁺, so the frequency of HDR is readily assayed by scoring the fraction of CD44⁺ (GFP⁺) cells. Figure 2F presents a representative example of an HDR assay that scores correction of the CD44 exon 17 mutation in HT1080 K1 cells.

Increased RECQ5 levels inhibit canonical HDR and stimulate alternative HDR

We first assayed effects of increased RECQ5 levels using the TL reporter stably integrated into the genome of human HEK 293T cells, an SV40-transformed cell line derived from embryonic kidney that is commonly used as a model for DNA repair (40,41,45–47). Ectopic expression of RECQ5 in 293T TL cells increased RECQ5 protein levels 15-fold (Supplementary Figure S3). DSBs and nicks were targeted to the TL reporter by CRISPR/Cas9 or CRISPR/Cas9^{D10A}, respectively. Canonical HDR was supported by the duplex plasmid donor pCVL SFFV d14GFP (40,41). Increased levels of RECQ5 inhibited RAD51-dependent canonical HDR by this duplex donor at both DSBs and nicks (Figure 3A), but stimulated alternative HDR at nicks by SSO donors (Figure 3B). The contrasting effects of RECQ5 expression on these two pathways are consistent with the ability of RECQ5 to disrupt RAD51 filaments, which will inhibit HDR supported by a duplex donor but stimulate HDR at nicks by SSO donors (40,41).

Stimulation of alternative HDR at nicks by increased RECQ5 levels did not depend upon the site of cleavage or whether repair occurred via the cI or cN pathway (as diagrammed in Figure 2A), as stimulation was evident at nicks targeted to three different sites in the TL reporter, repaired by donors complementary to either the intact or nicked strand (Figure 3C). Slightly different frequencies were evident at each site, probably reflecting both sensitivity of HDR to donor/target heterology (41) and sequence-dependent differences in cleavage and repair.

Stimulation of alternative HDR by RECQ5 depends upon RAD51/BRCA2 and is abrogated upon their depletion

If disruption of RAD51–DNA filaments is the mechanism by which increased levels of RECQ5 stimulate alternative HDR at nicks, then treatments that inhibit RAD51 loading or activity are predicted to abrogate stimulation. We tested this by assaying alternative HDR at nicks targeted by g1 and g9 and repaired by SSO donors using the cI and cN pathways. Control experiments showed that depletion of either RAD51 or BRCA2 stimulated alternative HDR at nicks at both sites, with frequencies reaching the 0.6–1.2% range (Figure 3C). However, depletion of either RAD51 or BRCA2 abrogated stimulation of alternative HDR at nicks in response to increased RECQ5 levels, as shown by comparison of relative HDR frequencies in cells treated with siNT2, siRAD51 or siBRCA2 for 24 h prior to ectopic expression of RECQ5 (Figure 3D). This is the result predicted if the mechanism by which RECQ5 stimulates alternative HDR is by dissociating RAD51 from DNA.

RECQ5 depletion inhibits alternative HDR by SSO donors

Depletion of RECQ5 by treatment of 293T TL cells with siRECQ5 reduced RECQ5 protein levels 3-fold (Supplementary Figure S3) and reduced frequencies of canonical HDR by dsDNA donors at both nicks and DSBs (Figure 4A). Inhibition of HDR at DSBs in response to RECQ5 depletion was anticipated by previous results (11). HDR that uses dsDNA donors depends upon RAD51 to promote strand invasion and D-loop formation [reviewed by (37)], and RECQ5 dissociates RAD51 filaments subsequent to synapsis (11). Depletion of RECQ5 may prevent dissociation of RAD51 from post-synaptic filaments, impairing their resolution.

RECQ5 depletion also reduced frequencies of alternative HDR by SSO donors at nicks in 293T TL cells (Figure 4B). If this reflects a requirement for the activity of RECQ5 at RAD51–DNA filaments, then the reduction should be abrogated upon depletion of RAD51 or BRCA2. This proved to be the case, as depletion of RECQ5 had no significant effect on HDR frequencies in 293T TL cells treated with either siRAD51 or siBRCA2 (Figure 4C).

The switch from canonical to alternative HDR requires RECQ5–RAD51 interaction

If RECQ5 promotes alternative HDR at nicks by disrupting RAD51 filaments, then stimulation of alternative HDR is predicted to depend on its interaction with RAD51. We

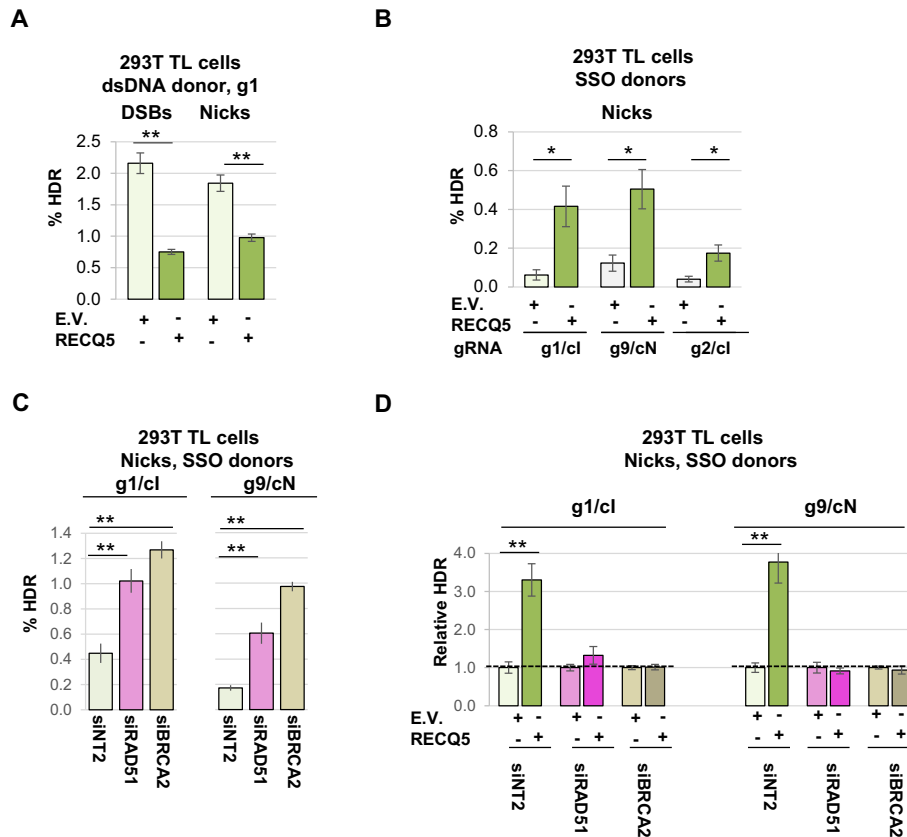


Figure 3. Contrasting response of canonical and alternative HDR to increased RECQ5 levels. In experiments shown in this figure, 293T TL cells were transiently transfected with E.V. or a vector for expression of siRECQ5-protected FLAG-RECQ5 (RECQ5), and with siRNAs as indicated. Reported HDR frequencies (% HDR) represent averages and standard errors of the mean of two separate experiments; $n \geq 6$. Significance measured by two-tailed T test. Significant differences are identified by asterisks: * indicates $P < 0.05$, ** indicates $P < 0.005$. (A) Response of frequencies of canonical HDR by dsDNA donors to increased RECQ5 levels. DSBs or nicks were targeted by g1. (B) Response of frequencies of HDR supported by SSO donors to increased RECQ5 levels. Nicks were targeted by g1, g9 or g2, as indicated. (C) Response of HDR frequencies to depletion of RAD51 or BRCA2 at nicks targeted by g1 (c1) or g9 (cN), as indicated. (D) Response of HDR frequencies to increased RECQ5 levels in cells depleted for RAD51 or BRCA2. Relative HDR was calculated for each pair of transfectants by normalizing frequencies in cells transfected with RECQ5 relative to E.V., indicated by a dotted line.

analyzed the importance of this interaction and other activities of RECQ5 by comparing HDR frequencies in 293T TL cells transiently transfected with wild-type RECQ5 and four different mutant derivatives (Figure 5A): RECQ5^{D157A}, which carries an active site mutation that abolishes helicase ATPase activity (11,48); RECQ5^{F666A}, which exhibits impaired interaction with RAD51 (10,11); and two mutants that affect transcription, RECQ5^{K598E}, defective in the region that competes with elongation factor TFIIS for binding to RNA Pol II; and RECQ5¹⁻⁸⁹⁹, which lacks the C-terminal domain that binds the phosphorylated CTD of elongating RNA Pol II (3,6,8,49). Control experiments showed that wild-type RECQ5 and its mutant derivatives were expressed at comparable levels, as assayed by western blotting with antibodies against the FLAG tag carried by constructs for ectopic expression (Supplementary Figure S4).

Increased levels of RECQ5 stimulated HDR 6-fold or more at nicks targeted to three different sites in the TL reporter in 293T TL cells (Figure 5B, left; Supplementary Data). In contrast, increased levels of RECQ5 inhibited HDR at DSBs (Figure 5B, right). Increased levels of wild-type RECQ5 stimulated HDR at nicks significantly more

than increased levels of RECQ5^{D157A} or RECQ5^{F666A}, so stimulation of HDR at nicks depended on helicase activity and RAD51 interactions (Figure 5B, left). Increased RECQ5¹⁻⁸⁹⁹ levels stimulated HDR even more than increased wild-type RECQ5 levels, suggesting that interactions with the Pol II CTD may inhibit stimulation, while increased levels of RECQ5^{K598E} stimulated HDR at nicks comparably to wild-type RECQ5 (Figure 5B).

At DSBs, inhibition of HDR depended upon helicase activity and to a lesser degree on RAD51 interaction, as no inhibition was evident upon expression of RECQ5^{D157A} and reduced inhibition was evident upon expression of RECQ5^{F666A} (Figure 5B, right). Expression of RECQ5 mutants with impaired interactions with RNA Pol II (RECQ5^{K598E} and RECQ5¹⁻⁸⁹⁹) caused a reduction in HDR significantly greater than that caused by expression of wild-type RECQ5, suggesting that Pol II interaction normally limits the ability of RECQ5 to act as an anti-recombinase at DSBs.

These results taken together with those in Figure 3 show that RECQ5 functions as an anti-recombinase in canonical HDR at DSBs, and that its anti-recombinase function de-

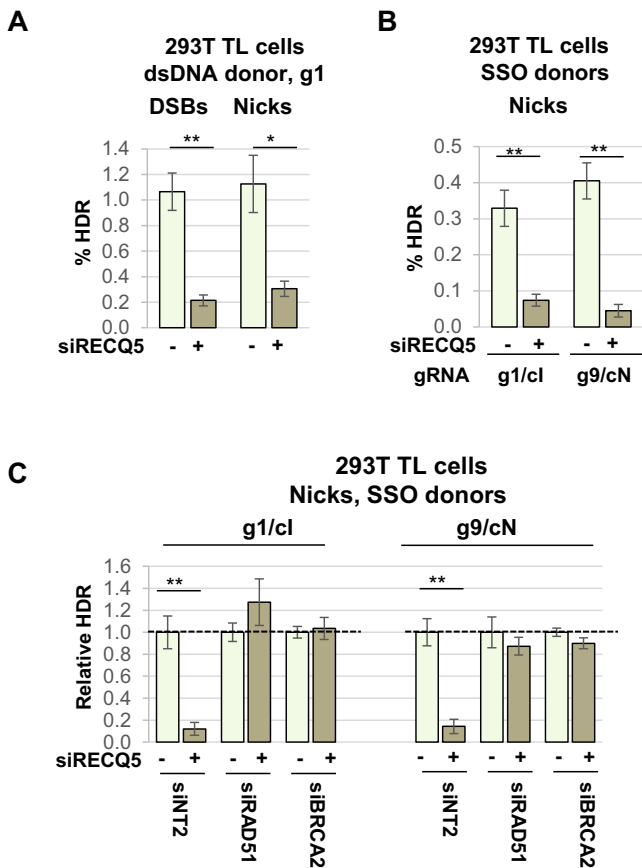


Figure 4. RECQ5 supports alternative HDR by counteracting BRCA2/RAD51. In experiments shown in this figure, 293T TL cells were treated with siRECQ5 or equivalent amounts of non-specific control siRNA, siINT2 (+ and -, respectively), and with additional siRNAs as indicated. Both absolute and relative HDR frequencies represent averages and standard errors of the mean of two separate experiments; $n \geq 6$. Significance measured by two-tailed T test. Significant differences are identified by asterisks: * indicates $P < 0.05$, ** indicates $P < 0.005$. (A) Response of frequencies of HDR by dsDNA donors to RECQ5 depletion. DSBs or nicks were targeted by g1. (B) Response of frequencies of HDR supported by SSO donors to RECQ5 depletion. Nicks were targeted by g1 (c1) or g9 (cN). (C) Relative frequencies of HDR at nicks targeted by indicated gRNAs and supported by indicated pathways, in 293T TL cells treated with siRECQ5, siINT2, siRAD51 or siBRCA2, as indicated. Relative HDR was calculated for each pair of transfectants by normalizing frequencies relative to the member of that pair in which RECQ5 was not depleted, indicated by a dotted line.

pend largely on its helicase ATPase activity and to lesser extent on RAD51 interactions. Interaction with Pol II appears to limit the anti-recombinase activity of RECQ5, raising the possibility that RECQ5 may contribute to preferential repair of DSBs at actively transcribed genes. Conversely, RECQ5 stimulates alternative HDR at nicks, and interactions with the Pol II CTD inhibit this stimulation and may thereby limit excess recombination at nicks in actively transcribed genes.

Increased RECQ5 levels stimulate mutEJ at nicks but not DSBs

We previously found that mutEJ frequencies at nicks, which are typically lower than at DSBs, are elevated by treatments

that diminish formation of RAD51–DNA filaments, such as depletion of BRCA2 or inhibition of RAD51 (40,41). This suggested that reduced or increased RECQ5 levels might affect mutEJ frequencies. To test this, we compared frequencies of mutEJ at nicks at three different target sites in 293T TL cells transiently transfected with E.V., RECQ5 or its mutant derivatives, normalizing mutEJ frequencies of mutant to wild-type RECQ5. This analysis showed that ectopic expression of RECQ5 stimulated mutEJ 4- to 18-fold relative to E.V., confirming the importance of RAD51 in preventing mutEJ at nicks (Figure 5C, left). At two of three sites tested (g1, g2, but not g9), the ability of RECQ5 to stimulate mutEJ was significantly reduced by mutation of its helicase or RAD51 interaction domain. The frequency of mutEJ at DSBs was at most modestly affected by ectopic expression of RECQ5 or its mutant derivatives (Figure 5C, right). These results support the notion that RAD51 binding to nicks can protect them from mutEJ and raise the possibility that tumors in which RECQ5 levels are elevated may experience greater levels of mutEJ at nicks, though not at DSBs.

Modulation of RECQ5 levels dysregulates repair in HT1080 human fibrosarcoma cells

We asked how modulations in RECQ5 levels affect HDR in a different cell type by analysis of HT1080 cells, a p53+ human fibrosarcoma line that proliferates with a predominantly diploid karyotype in culture. Depletion of BRCA2 stimulated HDR at nicks but inhibited HDR at DSBs in HT1080 TL cells (Figure 6A), as in 293T TL cells (compare Figure 3C). Thus, both the alternative and canonical HDR pathways are active in this cell type. Depletion of RECQ5, which reduced RECQ5 levels by 50% (Supplementary Figure S5), reduced HDR at both nicks and DSBs by more than 10-fold (Figure 6A), even more than in 293T cells (compare Figure 4A).

Ectopic expression of wild-type RECQ5 increased protein levels 1.9-fold in nuclear extracts of HT1080 cells (Supplementary Figure S5), but even this modest increase caused a significant stimulation of HDR at nicks targeted by g1 and supported by an SSO donor relative to E.V. (1.5-fold), and conversely diminished HDR at DSBs by dsDNA donors relative to E.V. (0.6-fold; Figure 6B). Dysregulation of HDR in response to alterations in RECQ5 levels appeared to depend upon RAD51 interactions, as the effect of ectopic expression of RECQ5^{F666A} on HDR frequencies at nicks was significantly below the effect of RECQ5 (Figure 6B, left). The effect of this mutation was not significant at DSBs (Figure 6B, right). Increased expression of RECQ5 stimulated mutEJ at nicks relative to E.V., and this stimulation depended upon RAD51 interaction, and increased expression of either RECQ5 or RECQ5^{F666A} modestly diminished mutEJ at DSBs (Figure 6C).

Depletion of BRCA2 or RECQ5 had pronounced effects on alternative and canonical HDR in HT1080 K1 cells very similar to those observed in HT1080 TL cells (compare Figure 6D and A). Assays of correction of the mutation in exon 17 of the endogenous CD44 gene in HT1080 K1 cells showed that HDR at nicks was stimulated nearly 2-fold by increased levels of wild-type RECQ5, just as at the TL re-

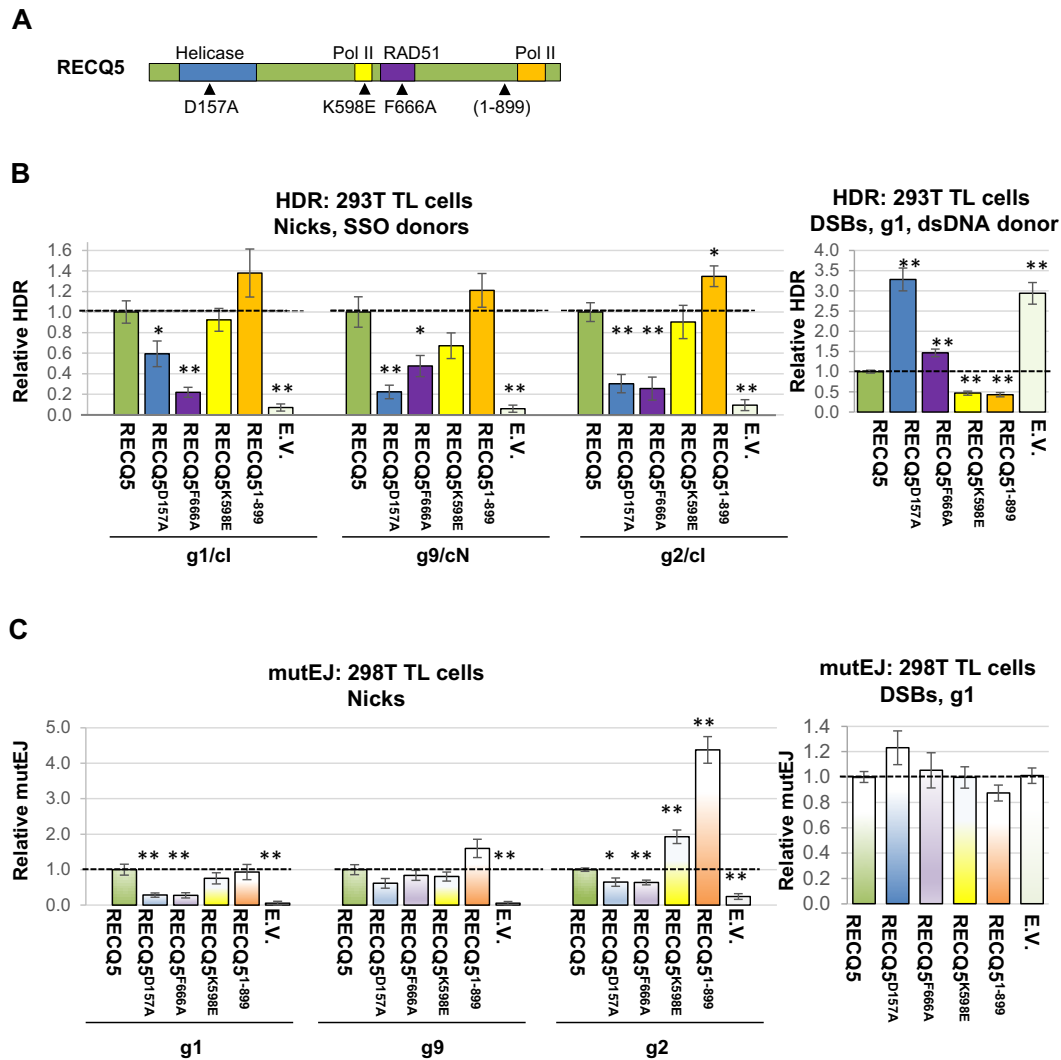


Figure 5. Stimulation of alternative HDR and mutEJ in 293T TL cells depends upon the RECQ5 helicase activity and RAD51 interaction domains. (A) Diagram of RECQ5, showing the helicase domain and the regions that interact with RAD51 or with RNA Pol II, and the mutations that disrupt the helicase ATPase (RECQ5^{D157A}), the RAD51 interaction domain (RECQ5^{F666A}) and the Pol II interaction domains (RECQ5^{K598E} and RECQ5¹⁻⁸⁹⁹). (B) Relative frequencies of HDR at nicks (left) or DSBs (right) targeted by indicated gRNAs and supported by indicated donors and pathways, in 293T TL cells treated with siRECQ5-St and transiently transfected with expression constructs for FLAG-RECQ5 (RECQ5), its derivatives bearing indicated mutations, or E.V. (C) Relative frequencies of mutEJ at nicks (left) or DSBs (right) targeted by indicated gRNAs in 293T TL cells treated with siRECQ5-St and transiently transfected with expression constructs for FLAG-RECQ5 (RECQ5), its derivatives bearing indicated mutations, or E.V. In panels (B) and (C), reported values represent averages and standard errors of the mean of two separate experiments; $n \geq 6$. Significance measured by two-tailed *T* test. Relative HDR frequencies were normalized to frequencies in RECQ5 transfectants, indicated by a dotted line. Significant differences relative to RECQ5 are indicated by asterisks: * indicates $P < 0.05$, ** indicates $P < 0.005$. Supplementary Data present statistics for other comparisons.

porter in HT1080 TL or 293T TL cells. This stimulation was dependent upon RAD51 interaction, as stimulation by RECQ5^{F666A} was significantly reduced relative to stimulation by RECQ5 (Figure 6E). These results show that even modest changes in RECQ5 levels can have significant effects on HDR frequencies.

DISCUSSION

The results reported here show that increased RECQ5 levels can have profound effects on repair pathway choice and on repair frequencies. Increased RECQ5 levels inhibited canonical HDR by exogenous dsDNA donors at DSBs and nicks and stimulated alternative HDR at nicks by ss-

DNA donors (Figure 3). Thus, increased levels of RECQ5 can promote the switch from canonical HDR to this alternative HDR pathway. Frequencies of alternative HDR at nicks were stimulated as much as 7-fold upon ectopic RECQ5 expression. Increased RECQ5 levels have also been reported to cause a modest (1.5-fold) increase in HDR by the single-strand annealing pathway (11), overcoming the normal suppression of this pathway by RAD51. Thus, increased RECQ5 levels phenocopy the effects of deficiencies in BRCA2 or other factors in the canonical HDR pathway. Tumors that are deficient in BRCA-dependent HDR are candidates for therapies that exploit this deficiency (50). Our results suggest that RECQ5 amplification may be a use-

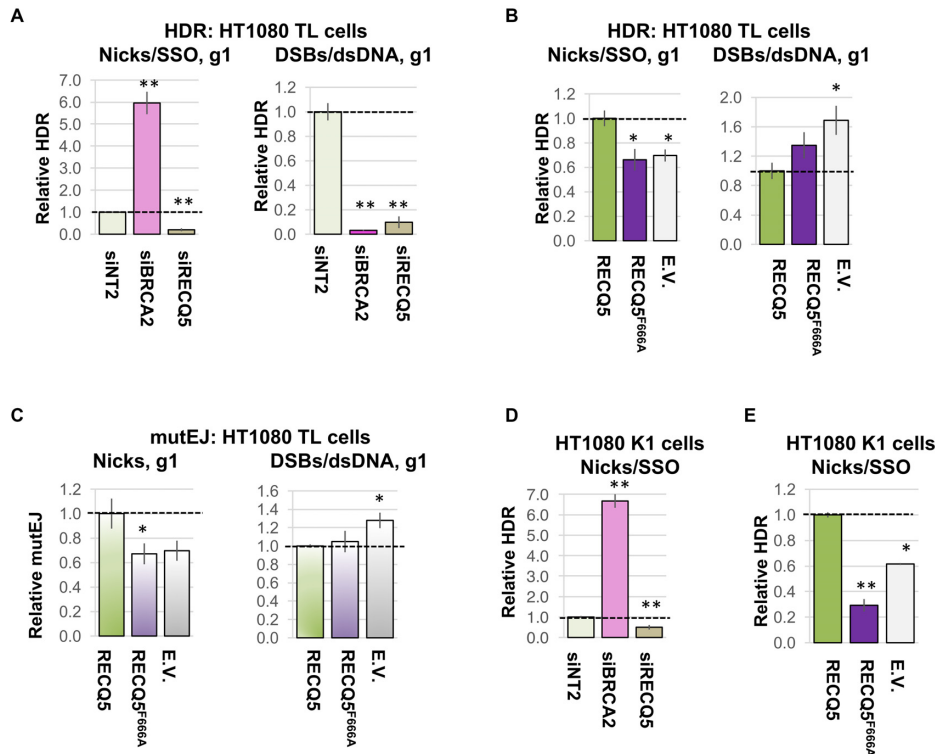


Figure 6. Modulation of RECQ5 levels dysregulates repair in HT1080 fibrosarcoma cells. (A) Relative frequencies of HDR at nicks (left) and DSBs (right) targeted by g1 in HT1080 TL cells in which BRCA2 or RECQ5 had been depleted. Significant differences relative to siNT2 control are indicated by asterisks: ** indicates $P < 0.005$. (B) Relative frequencies of HDR at nicks (left) and DSBs (right) targeted by g1 in HT1080 TL cells transiently transfected with expression constructs for FLAG-RECQ5 (RECQ5), its derivative bearing a mutation in the RAD51 interaction domain (RECQ5^{F666A}), or E.V. Relative HDR frequencies were normalized to frequencies in cells transfected with RECQ5, indicated by a dotted line. Significant differences relative to RECQ5 are indicated by asterisks: * indicates $P < 0.05$. (C) Relative frequencies of mutEJ at nicks (left) or DSBs (right) targeted by g1 in HT1080 TL cells transiently transfected with expression constructs for FLAG-RECQ5 (RECQ5), its derivative bearing a mutation in the RAD51 interaction domain (RECQ5^{F666A}), or E.V. Relative mutEJ frequencies were normalized to frequencies in cells transfected with RECQ5, indicated by a dotted line. Significant differences relative to RECQ5 are indicated by asterisks: * indicates $P < 0.05$. (D) Relative frequencies of HDR at nicks targeted to CD44 exon 17 by gRNA-CD44T-17-2 and supported by SSO donor SSO-CD44T-17-0 in HT1080 K1 cells in which BRCA2 or RECQ5 had been depleted. Significant differences relative to siNT2 control are indicated by asterisks: ** indicates $P < 0.005$. (E) Relative frequencies of HDR at nicks targeted to CD44 exon 17 by gRNA-CD44T-17-2 and supported by SSO donor SSO-CD44T-17-0 in HT1080 K1 cells transiently transfected with expression constructs for FLAG-RECQ5 (RECQ5), its derivative bearing a mutation in the RAD51 interaction domain (RECQ5^{F666A}), or E.V. Relative HDR frequencies were normalized to frequencies in cells transfected with RECQ5, indicated by a dotted line. Significant differences relative to RECQ5 are indicated by asterisks: ** indicates $P < 0.005$.

ful biomarker for identification of tumors that phenocopy ‘BRCA-ness’.

The RECQ5-driven switch from canonical to alternative HDR at nicks occurred in conditions permissive for RAD51–DNA filament formation, but not in cells depleted for either RAD51 or BRCA2. The switch depended upon RECQ5 helicase activity and upon the RECQ5–RAD51 interaction, which are essential to disruption of RAD51 filaments *in vitro* by RECQ5 (4,10). Thus, disruption of RAD51–DNA filaments by RECQ5 helicase is likely to be the mechanism by which RECQ5 stimulates the switch from canonical to alternative HDR.

Figure 7 diagrams the shift from canonical to alternative HDR that occurs at nicks in response to elevated RECQ5 levels. Unwinding or excision of a nick generates a single-stranded region that is bound by RAD51, which forms filaments on the exposed single-stranded regions that enable invasion of a duplex donor and repair by canonical HDR. RAD51 binding inhibits annealing to the exogenous ssDNA donor that supports alternative HDR, and RECQ5 dissociates RAD51 from DNA and enables annealing to a

ssDNA donor DNA, thereby promoting alternative HDR. This activity of RECQ5 would promote HDR via both the cN and cI pathways, which respond similarly to increased RECQ5 levels.

Ectopic expression of RECQ5 inhibited canonical HDR at DSBs. This anti-recombinase role depended largely on its helicase ATPase activity and to lesser extent on RAD51 interactions. RECQ5 interacts not only with RAD51 but also with Pol II, and interaction with Pol II appears to limit the anti-recombinase activity of RECQ5, raising the possibility that interactions of RECQ5 with Pol II may contribute to preferential repair of DSBs at actively transcribed genes. Interactions with the Pol II CTD also inhibit stimulation of alternative HDR at nicks. Nicks can accumulate in actively transcribed genes to modulate superhelicity, and RECQ5/Pol II interactions may limit recombination that could accompany active transcription.

Increased levels of RECQ5 stimulated frequencies of mutEJ at nicks but not DSBs (Figures 5C and 6C). The effects of increased and decreased levels of RECQ5 on mutEJ at nicks paralleled effects on alternative HDR fre-

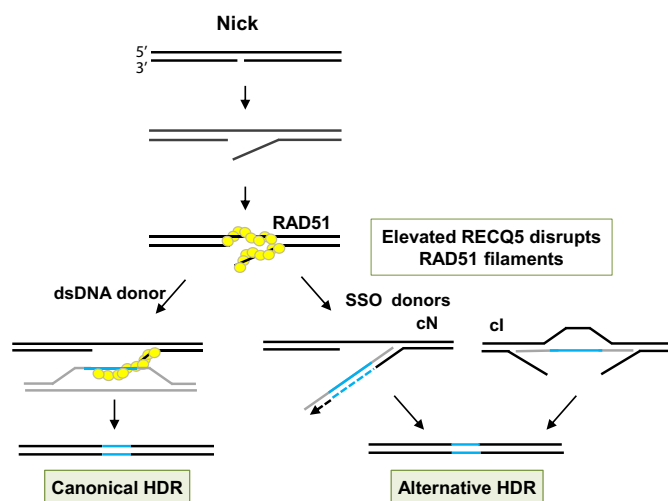


Figure 7. How increased RECQ5 levels may promote a shift from canonical to alternative HDR. A nick is unwound, and then bound by RAD51, which is loaded onto DNA by BRCA2. In canonical HDR (left), RAD51 filaments at the end of the target promote invasion of a DNA duplex donor. Increased RECQ5 levels disrupt RAD51 filaments to promote alternative HDR (right), in which a ssDNA donor anneals to the target.

quencies at nicks (Figures 3 and 4). Stimulation depended upon the ability of RECQ5 to disrupt RAD51 filaments. The frequency of mutEJ at nicks is also stimulated by other treatments that diminish formation or stability of RAD51–DNA filaments, including depletion of RAD51, BRCA2 or BRCA2 binding partners, or expression of dominant negative RAD51 or the inhibitory BRC3 peptide (40,41). These results further support the view that RAD51 binding to nicks protects them from mutEJ. They also make it unlikely that the strategy of stimulating alternative HDR by transient increases in RECQ5 levels could be useful for genome engineering, unless methods could be developed for preventing the concomitant stimulation of mutEJ. Strategies employing RECQ5 to stimulate gene correction may emerge from more detailed understanding of the mechanism of mutEJ at nicks.

Alteration of RECQ5 levels dysregulates HDR

RECQ5 levels appeared to be closely regulated in both HT1080 and 293T cells. Depletion that caused only modest reductions in RECQ5 levels (2- and 3-fold, respectively) reduced HDR frequencies in both cell types, especially HT1080. Moreover, ectopic expression that increased protein levels only 2-fold in HT1080 cells caused a significant increase in alternative HDR at nicks accompanied by a decrease in canonical HDR at DSBs.

RECQ5 is frequently amplified in tumors, and analysis of 32 tumor types (over 9000 individual tumors) showed that increased expression correlates with gene amplification (Figure 1). In some tumors, effects of increased RECQ5 expression appear to be compensated by—or compensate for—dysregulated expression of other genes. We observed a positive correlation between expression of RECQ5 and SHFM1(DSS1) (Figure 1). SHFM1(DSS1) binds and stabilizes BRCA2, and positive correlation of RECQ5 and

SHFM1(DSS1) expression in tumors could overcome dissociation of RAD51 filaments caused by increased RECQ5 levels to promote genomic stability. In contrast, we observed a negative correlation between expression of RECQ5 and RAD51 or BRCA2 (Figure 1). This negative correlation could reflect selective pressure for the switch from canonical to alternative HDR in response to either increased RECQ5 or decreased RAD51 or BRCA2 levels, which may contribute to genomic instability and aggressive malignancy. Levels of RAD51 are also frequently elevated in tumors (51) and this can stabilize RAD51 filaments (52), giving rise to a suggestion that increased RECQ5 levels might be able to counteract high levels of RAD51 to avoid excess recombination (2). However, the negative correlation between RECQ5 and RAD51 expression suggests that this may be uncommon. Conversely, the possibility that it may be useful to develop drugs that inhibit RECQ5 was suggested by examination of myeloproliferative neoplasms, where increased levels of RECQ5 overcome replication stress to diminish sensitivity to hydroxyurea, the most common treatment for this disease (22). The evidence that reduced levels of RECQ5 inhibit HDR (Figure 4) raises the caveat that cells that survive treatments with such drugs may exhibit elevated genomic instability.

RECQ5, BLM and FANCD1 employ their helicase ATPase activity to dissociate RAD51–DNA filaments. Like RECQ5 (but not WRN), amplification is the predominant alteration of the BLM and FANCD1 genes in many tumors (Figure 1A and Supplementary Figure S1). It will be interesting to learn whether increased expression of BLM and FANCD1 can cause a shift from canonical to alternative HDR analogous to the one we have documented for RECQ5.

SUPPLEMENTARY DATA

Supplementary Data are available at NAR Online.

ACKNOWLEDGEMENTS

We thank members of the Maizels lab for insights and comments, and Donna Prunkard for help with flow cytometry. The results reported here are in part based upon data generated by the TCGA Research Network: <http://cancergenome.nih.gov/>.

FUNDING

National Cancer Institute of the National Institutes of Health under award numbers [R01 CA183967 (to N.M.), P01 CA077852 (to N.M. and T.K.), R01 CA130910 (to Y.L.)]; National Institute of General Medical Sciences of the National Institutes of Health training grants [T32 GM095421, T32 GM007270] and a Howard Hughes Medical Institute-University of Washington Molecular Medicine Scholar Award (to H.C.O.). Funding for open access charge: NIH [P01 CA077852].

Conflict of interest statement. None declared.

REFERENCES

- Zheng, L., Kanagaraj, R., Mihaljevic, B., Schwendener, S., Sartori, A.A., Gerrits, B., Shevelev, I. and Janscak, P. (2009) MRE11

- complex links RECQ5 helicase to sites of DNA damage. *Nucleic Acids Res.*, **37**, 2645–2657.
2. Di Marco, S., Hasanova, Z., Kanagaraj, R., Chappidi, N., Altmannova, V., Menon, S., Sedlackova, H., Langhoff, J., Surendranath, K., Huhn, D. *et al.* (2017) RECQ5 helicase cooperates with MUS81 endonuclease in processing stalled replication forks at common fragile sites during mitosis. *Mol. Cell*, **66**, 658–671.
 3. Saponaro, M., Kantidakis, T., Mitter, R., Kelly, G.P., Heron, M., Williams, H., Söding, J., Stewart, A. and Svejstrup, J.Q. (2014) RECQL5 controls transcript elongation and suppresses genome instability associated with transcription stress. *Cell*, **157**, 1037–1049.
 4. Hu, Y., Raynard, S., Sehorn, M.G., Lu, X., Bussen, W., Zheng, L., Stark, J.M., Barnes, E.L., Chi, P., Jancsak, P. *et al.* (2007) RECQL5/Recql5 helicase regulates homologous recombination and suppresses tumor formation via disruption of Rad51 presynaptic filaments. *Genes Dev.*, **21**, 3073–3084.
 5. Aygün, O., Svejstrup, J. and Liu, Y. (2008) A RECQ5-RNA polymerase II association identified by targeted proteomic analysis of human chromatin. *Proc. Natl. Acad. Sci. U.S.A.*, **105**, 8580–8584.
 6. Aygün, O., Xu, X., Liu, Y., Takahashi, H., Kong, S.E., Conaway, R.C., Conaway, J.W. and Svejstrup, J.Q. (2009) Direct inhibition of RNA polymerase II transcription by RECQL5. *J. Biol. Chem.*, **284**, 23197–23203.
 7. Kanagaraj, R., Huehn, D., MacKellar, A., Menigatti, M., Zheng, L., Urban, V., Shevelev, I., Greenleaf, A.L. and Jancsak, P. (2010) RECQ5 helicase associates with the C-terminal repeat domain of RNA polymerase II during productive elongation phase of transcription. *Nucleic Acids Res.*, **38**, 8131–8140.
 8. Li, M., Xu, X. and Liu, Y. (2011) The SET2-RPB1 interaction domain of human RECQ5 is important for transcription-associated genome stability. *Mol. Cell Biol.*, **31**, 2090–2099.
 9. Li, M., Pokharel, S., Wang, J.T., Xu, X. and Liu, Y. (2015) RECQ5-dependent SUMOylation of DNA topoisomerase I prevents transcription-associated genome instability. *Nat. Commun.*, **6**, 6720.
 10. Schwendener, S., Raynard, S., Paliwal, S., Cheng, A., Kanagaraj, R., Shevelev, I., Stark, J.M., Sung, P. and Jancsak, P. (2010) Physical interaction of RECQ5 helicase with RAD51 facilitates its anti-recombinase activity. *J. Biol. Chem.*, **285**, 15739–15745.
 11. Paliwal, S., Kanagaraj, R., Sturzenegger, A., Burdova, K. and Jancsak, P. (2014) Human RECQ5 helicase promotes repair of DNA double-strand breaks by synthesis-dependent strand annealing. *Nucleic Acids Res.*, **42**, 2380–2390.
 12. Kowalczykowski, S.C. (2015) An overview of the molecular mechanisms of recombinational DNA repair. *Cold Spring Harb. Perspect. Biol.*, **7**, a016410.
 13. Khadka, P., Croteau, D.L. and Bohr, V.A. (2016) RECQL5 has unique strand annealing properties relative to the other human RecQ helicase proteins. *DNA Repair*, **37**, 53–66.
 14. Bugreev, D.V., Yu, X., Egelman, E.H. and Mazin, A.V. (2007) Novel pro- and anti-recombination activities of the Bloom's syndrome helicase. *Genes Dev.*, **21**, 3085–3094.
 15. Sommers, J.A., Rawtani, N., Gupta, R., Bugreev, D.V., Mazin, A.V., Cantor, S.B. and Brosh, R.M. Jr (2009) FANCD1 uses its motor ATPase to destabilize protein-DNA complexes, unwind triplexes, and inhibit RAD51 strand exchange. *J. Biol. Chem.*, **284**, 7505–7517.
 16. Tadokoro, T., Ramamoorthy, M., Popuri, V., May, A., Tian, J., Sykora, P., Rybanska, I., Wilson, D.M. 3rd, Croteau, D.L. and Bohr, V.A. (2012) Human RECQL5 participates in the removal of endogenous DNA damage. *Mol. Biol. Cell*, **23**, 4273–4285.
 17. Popuri, V., Ramamoorthy, M., Tadokoro, T., Singh, D.K., Karmakar, P., Croteau, D.L. and Bohr, V.A. (2012) Recruitment and retention dynamics of RECQL5 at DNA double strand break sites. *DNA Repair*, **11**, 624–635.
 18. Popuri, V., Huang, J., Ramamoorthy, M., Tadokoro, T., Croteau, D.L. and Bohr, V.A. (2013) RECQL5 plays co-operative and complementary roles with WRN syndrome helicase. *Nucleic Acids Res.*, **41**, 881–899.
 19. Croteau, D.L., Popuri, V., Opreko, P.L. and Bohr, V.A. (2014) Human RecQ helicases in DNA repair, recombination, and replication. *Annu. Rev. Biochem.*, **83**, 519–552.
 20. Cerami, E., Gao, J., Dogrusoz, U., Gross, B.E., Sumer, S.O., Aksoy, B.A., Jacobsen, A., Byrne, C.J., Heuer, M.L., Larsson, E. *et al.* (2012) The cBio cancer genomics portal: an open platform for exploring multidimensional cancer genomics data. *Cancer Discov.*, **2**, 401–404.
 21. Gao, J., Aksoy, B.A., Dogrusoz, U., Dresdner, G., Gross, B., Sumer, S.O., Sun, Y., Jacobsen, A., Sinha, R., Larsson, E. *et al.* (2013) Integrative analysis of complex cancer genomics and clinical profiles using the cBioPortal. *Sci. Signal.*, **6**, doi:10.1126/scisignal.2004088.
 22. Chen, E., Ahn, J.S., Sykes, D.B., Breyfogle, L.J., Godfrey, A.L., Nangalia, J., Ko, A., DeAngelo, D.J., Green, A.R. and Mullally, A. (2015) RECQL5 suppresses oncogenic JAK2-induced replication stress and genomic instability. *Cell Rep.*, **13**, 2345–2352.
 23. Arora, A., Abdel-Fatah, T.M., Agarwal, D., Doherty, R., Croteau, D.L., Moseley, P.M., Hameed, K., Green, A., Aleskandarany, M.A., Rakha, E.A. *et al.* (2016) Clinicopathological and prognostic significance of RECQL5 helicase expression in breast cancers. *Carcinogenesis*, **37**, 63–71.
 24. Patterson, K., Arya, L., Bottomley, S., Morgan, S., Cox, A., Catto, J. and Bryant, H.E. (2016) Altered RECQL5 expression in urothelial bladder carcinoma increases cellular proliferation and makes RECQL5 helicase activity a novel target for chemotherapy. *Oncotarget*, **7**, 76140–76150.
 25. Heyer, W.D., Ehmsen, K.T. and Liu, J. (2010) Regulation of homologous recombination in eukaryotes. *Annu. Rev. Genet.*, **44**, 113–139.
 26. Symington, L.S. and Gautier, J. (2011) Double-strand break end resection and repair pathway choice. *Annu. Rev. Genet.*, **45**, 247–271.
 27. Jasin, M. and Rothstein, R. (2013) Repair of strand breaks by homologous recombination. *Cold Spring Harb. Perspect. Biol.*, **5**, a012740.
 28. Jasin, M. and Haber, J.E. (2016) The democratization of gene editing: Insights from site-specific cleavage and double-strand break repair. *DNA Repair*, **44**, 6–16.
 29. San Filippo, J., Sung, P. and Klein, H. (2008) Mechanism of eukaryotic homologous recombination. *Annu. Rev. Biochem.*, **77**, 229–257.
 30. Colavito, S., Prakash, R. and Sung, P. (2010) Promotion and regulation of homologous recombination by DNA helicases. *Methods*, **51**, 329–335.
 31. Taylor, M.R., Spirek, M., Chaurasiya, K.R., Ward, J.D., Carzaniga, R., Yu, X., Egelman, E.H., Collinson, L.M., Rueda, D., Krejci, L. *et al.* (2015) Rad51 paralogs remodel pre-synaptic Rad51 filaments to stimulate homologous recombination. *Cell*, **162**, 271–286.
 32. Bell, J.C. and Kowalczykowski, S.C. (2016) RecA: regulation and mechanism of a molecular search engine. *Trends Biochem. Sci.*, **41**, 491–507.
 33. Godin, S.K., Sullivan, M.R. and Bernstein, K.A. (2016) Novel insights into RAD51 activity and regulation during homologous recombination and DNA replication. *Biochem. Cell Biol.*, **94**, 407–418.
 34. Haber, J.E. (2016) A life investigating pathways that repair broken chromosomes. *Annu. Rev. Genet.*, **50**, 1–28.
 35. Morrical, S.W. (2015) DNA-pairing and annealing processes in homologous recombination and homology-directed repair. *Cold Spring Harb. Perspect. Biol.*, **7**, a016444.
 36. Sfeir, A. and Symington, L.S. (2015) Microhomology-mediated end joining: a back-up survival mechanism or dedicated pathway? *Trends Biochem. Sci.*, **40**, 701–714.
 37. Bhargava, R., Onyango, D.O. and Stark, J.M. (2016) Regulation of single-strand annealing and its role in genome maintenance. *Trends Genet.*, **32**, 566–575.
 38. Ceccaldi, R., Rondinelli, B. and D'Andrea, A.D. (2016) Repair pathway choices and consequences at the double-strand break. *Trends Cell Biol.*, **26**, 52–64.
 39. Verma, P. and Greenberg, R.A. (2016) Noncanonical views of homology-directed DNA repair. *Genes Dev.*, **30**, 1138–1154.
 40. Davis, L. and Maizels, N. (2014) Homology-directed repair of DNA nicks via pathways distinct from canonical double-strand break repair. *Proc. Natl. Acad. Sci. U.S.A.*, **111**, E924–E932.
 41. Davis, L. and Maizels, N. (2016) Two distinct pathways support gene correction by single-stranded donors at DNA nicks. *Cell Rep.*, **17**, 1872–1881.
 42. Certo, M.T., Ryu, B.Y., Annis, J.E., Garibov, M., Jarjour, J., Rawlings, D.J. and Scharenberg, A.M. (2011) Tracking genome engineering outcome at individual DNA breakpoints. *Nat. Methods*, **8**, 671–676.

43. Mali,P., Yang,L., Esvelt,K.M., Aach,J., Guell,M., DiCarlo,J.E., Norville,J.E. and Church,G.M. (2013) RNA-guided human genome engineering via Cas9. *Science*, **339**, 823–826.
44. Davis,L., Zhang,Y. and Maizels,N. (2018) Assaying Repair at DNA Nicks. *Methods Enzymol.*, **601**, 71–89.
45. Cong,L., Ran,F.A., Cox,D., Lin,S., Barretto,R., Habib,N., Hsu,P.D., Wu,X., Jiang,W., Marraffini,L.A. *et al.* (2013) Multiplex genome engineering using CRISPR/Cas systems. *Science*, **339**, 819–823.
46. Richardson,C.D., Ray,G.J., Bray,N.L. and Corn,J.E. (2016) Non-homologous DNA increases gene disruption efficiency by altering DNA repair outcomes. *Nat. Commun.*, **7**, 12463.
47. Bothmer,A., Phadke,T., Barrera,L.A., Margulies,C.M., Lee,C.S., Buquicchio,F., Moss,S., Abdulkarim,H.S., Selleck,W., Jayaram,H. *et al.* (2017) Characterization of the interplay between DNA repair and CRISPR/Cas9-induced DNA lesions at an endogenous locus. *Nat. Commun.*, **8**, 13905.
48. Ozsoy,A.Z., Ragonese,H.M. and Matson,S.W. (2003) Analysis of helicase activity and substrate specificity of *Drosophila* RECQ5. *Nucleic Acids Res.*, **31**, 1554–1564.
49. Kassube,S.A., Jinek,M., Fang,J., Tsutakawa,S. and Nogales,E. (2013) Structural mimicry in transcription regulation of human RNA polymerase II by the DNA helicase RECQL5. *Nat. Struct. Mol. Biol.*, **20**, 892–899.
50. Lord,C.J. and Ashworth,A. (2016) BRCAness revisited. *Nat. Rev. Cancer*, **16**, 110–120.
51. Klein,H.L. (2008) The consequences of Rad51 overexpression for normal and tumor cells. *DNA Repair*, **7**, 686–693.
52. Schlacher,K., Wu,H. and Jasin,M. (2012) A distinct replication fork protection pathway connects Fanconi anemia tumor suppressors to RAD51-BRCA1/2. *Cancer Cell*, **22**, 106–116.